Optics & Laser Technology 65 (2015) 131–136

Contents lists available at ScienceDirect

Optics & Laser Technology

journal homepage: www.elsevier.com/locate/optlastec

Temperature and axial strain characteristic of cladding etched single-mode fiber based acousto-optic tunable filter

Chao Liu, Li Pei*, Yiqun Wang, Sijun Weng, Liangying Wu, Shaowei Yu

Key Laboratory of All Optical Network and Advanced Telecommunication Network of Ministry of Education, Institute of Lightwave Technology, Beijing Jiaotong University, Beijing 100044, China

ARTICLE INFO

Article history:
Received 20 April 2014
Received in revised form
9 July 2014
Accepted 14 July 2014
Available online 12 August 2014

Keywords:
Acousto-optic tunable filter
Temperature
Axial strain

ABSTRACT

The temperature and axial strain characteristic of the cladding etched single-mode fiber based acousto-optic tunable filter (CE-SMF-AOTF) were described in the simulation and experiment. In the simulation, the CE-SMF-AOTF had a linear wavelength shift response to the temperature and axial strain, and the filter with small fiber diameter was more sensitive to the temperature and axial strain than it with large fiber diameter. In the experiment, the temperature and axial strain characteristic of the CE-SMF-AOTF with fiber diameters of 39 μm and 67 μm were measured. The experimental results accorded well with the simulated ones.

1. Introduction

Optical filters are key components for optical communication systems. Due to their tunable spectra, the filters can be used in optical signal processing [1], wavelength selection [2] and optical amplifiers [3]. Currently, the common optical filters include fiber gratings [4–6], acousto-optic tunable filters (AOTFs) [2], Mach–Zehnder interferometer filters [7], Fabry–Perot filters [8] and so on. Among these tunable filters, the AOTFs have the advantages of wide tunable range, good switching speed, and easy electric control. Particularly, all-fiber AOTFs have good compatibility with optical fiber communication systems. Therefore, there is a lively interest in the design of all-fiber AOTFs to obtain tunable complex spectra. In 1997, an all-fiber AOTF based on single-mode fiber (SMF) was first demonstrated by Kim et al. [9], and in order to enhance the coupling efficiency, Li et al. designed a cladding etched SMF based AOTF (CE-SMF-AOTF) in 2002 [10]. Other types of all-fiber AOTFs are also proposed with the components such as taper fiber [11] and fiber grating [12,13]. For the application of these all-fiber AOTFs, it is significant to understand the effects of various external perturbations such as temperature fluctuation and axial strain on the device performance. It is because the temperature and axial strain characteristic of the filter largely determine its packaging structure. There have been a few reports on the axial strain characteristics of some all-fiber AOTFs [14–17]. In 2006, Li et al. analyzed the axial strain characteristic of the fiber taper based AOTF [15], but the variation of the fiber which is induced by the strain, is negligible. In 2009, Lee et al. reported the axial strain characteristic of SMF based AOTF by consideration of the combination of acoustic and optical effects [16], but the variation of the fiber diameter has not been fully considered in the analysis of this AOTF. To the best of our knowledge, no report was appeared on the temperature characteristic of the CE-SMF-AOTF.

In this paper, the temperature and axial strain characteristic of the CE-SMF-AOTF with different fiber diameters are demonstrated in the simulation and experiment. In the simulation, the optical resonant wavelength shift of the filter is explained by the combination of the acoustic and optical effect in the fiber which are significantly affected by the temperature and axial strain. In the experiment, the filter with different diameters are measured under several temperatures and axial strains.

2. Operation of the CE-SMF-AOTF

As shown in Fig. 1, the CE-SMF-AOTF is composed of the cladding-etched single mode fiber, the silica horn and the PZT. When the electrical signal is loaded on the PZT, the PZT vibrates up and down, creating a flexural acoustic wave in the fiber. After propagating over the acousto-optic (AO) interaction region where the fiber cladding is etched, the flexural acoustic wave is absorbed by the fiber coating layer. The flexural acoustic wave bends the fiber and changes the refractive index distribution of the fiber, periodically. When the fiber is assumed to vibrate in the *yz* plane (vertical plane), the change of the refractive index Δn can be

* Corresponding author.
E-mail address: lipei@bjtu.edu.cn (L. Pei).

http://dx.doi.org/10.1016/j.optlastec.2014.07.012
0030-3992/

expressed as [11]

$$\Delta n(x,y,z) = n_0(1+\chi)k_a^2 S_0 y \cos(k_a z) \quad (1)$$

where n_0 is the effective local index, χ is the elasto-optic contribution to the index change, $k_a = 2\pi/\Lambda_a$ is the vector of the acoustic wave, S_0 is the amplitude of the flexural acoustic wave, and Λ_a is the acoustic wavelength.

The change of the refractive index in the fiber causes the coupling from the HE_{11} mode in the core to the HE_{21} mode in the cladding at the resonant wavelength where the phase matching condition is satisfied: the acoustic wavelength $\Lambda_a$should be the same as the optical beat-length L_B between the core mode HE_{11} and the cladding mode HE_{21} [14],

$$\Lambda_a = L_B = \frac{2\pi}{\beta_{11}-\beta_{21}} \quad (2)$$

where β_{11} and β_{21} are the propagation constants of the core mode HE_{11} and the cladding mode HE_{21}, respectively.

Then the HE_{21} mode is absorbed by the fiber coating layer, giving rise to a wavelength notch in the transmission spectra. The coupled mode equations between the HE_{11} mode and the HE_{21} mode can be given by [11]

$$\frac{dE_{11}}{dz} + iK_s e^{i\delta_s z}E_{21} = 0,\ \frac{dE_{21}}{dz} + iK_s e^{-i\delta_s z}E_{11} = 0 \quad (3)$$

where E_{11} and E_{21} are mode field intensity of the HE_{11} mode and the HE_{21} mode respectively, K_s is the AO coupling coefficient, and $\delta_s = \beta_{11}-\beta_{21}-2\pi/\Lambda_a$ is a detuning parameter that is zero at the optical resonant wavelength, respectively.

3. The temperature characteristic of the CE-SMF-AOTF

When the temperature of the CE-SMF-AOTF varies, the acoustic wavelength Λ_a and the optical beat-length L_B change, leading to the shift of the optical resonant wavelength. In a cylindrical optical fiber, the fiber diameter is much smaller than the acoustic wavelength of lowest order flexural acoustic wave. Therefore, the frequency f_a of the flexural acoustic wave can be expressed as [16]

$$f_a = \frac{2\pi}{\Lambda_a^2}\left[\left(\frac{E_a I_a}{\rho S}\right)\left(1+\frac{\Lambda_a^2 T_a}{4\pi^2 E_a I_a}\right)\right]^{1/2} \quad (4)$$

where E_a, I_a, ρ, S and T_a are Young's modulus, the area moment of inertia, the fiber density, the cross-sectional area of the fiber, and the initial tension in the longitudinal direction of the fiber, respectively. When the temperature changes ΔT, because the area moment of inertia and the initial tension can be given by

$$I_a = \frac{\pi}{4}\left(\frac{d}{2}\right)^4,\quad T_a = E_a S\frac{\Delta l}{l} = E_a S\alpha\Delta T, \quad (5)$$

respectively, the acoustic wavelength Λ_a of the lowest order flexural acoustic wave can be expressed as

$$\Lambda_a = \frac{C_{ext}}{\sqrt{2}f_a}\sqrt{\alpha\Delta T + \sqrt{(\alpha\Delta T)^2 + \left(\frac{\pi f_a}{C_{ext}}(1+\alpha\Delta T)d\right)^2}} \quad (6)$$

where C_{ext} is the speed of the acoustic wave in fiber, f_a is the acoustic frequency, α is the thermal expansion coefficient of the fiber, and d is the fiber diameter. For silica, the values of C_{ext} and α are about 5760 m/s and $5.5\times10^{-7}/^{o}$C, respectively.

Based on Eq. (6), the relationship between the acoustic wavelength Λ_a and the fiber diameter d can be obtained, as shown in Fig. 2. In the simulation, the acoustic frequency f_a is 0.9 MHz. The graph shows that the acoustic wavelength decreases with the decrease of the fiber diameter, and when the temperature increases, the acoustic wavelength also increases.

When the temperature changes ΔT, the parameters of the fiber varies. According to the thermal expansion effect and thermo-optic effect, the radius and refractive index of fiber core and fiber cladding are changed as [18]:

for the fiber core,

$$r^{co} = r_0^{co}(1+\alpha\Delta T),\quad n^{co} = n_0^{co}(1+\zeta^{co}\Delta T), \quad (7)$$

for the fiber cladding,

$$r^{cl} = r_0^{cl}(1+\alpha\Delta T),\quad n^{cl} = n_0^{cl}(1+\zeta^{cl}\Delta T), \quad (8)$$

where r_0^{co} and r_0^{cl} are the initial radius of the fiber core and fiber cladding, n_0^{co} and n_0^{cl} are the initial refractive index of the fiber core and fiber cladding, ζ^{co} and ζ^{cl} are the thermo-optic coefficient of the fiber core and fiber cladding, respectively.

Fig. 3 shows the relationship between the effective refractive index of the fiber mode (HE_{11} and HE_{12}) and the fiber diameter d. The calculation is based on Eqs. (7) and (8), and the characteristic equation for the core mode and the cladding mode which are obtained from the step-index fiber geometry [19]. In the

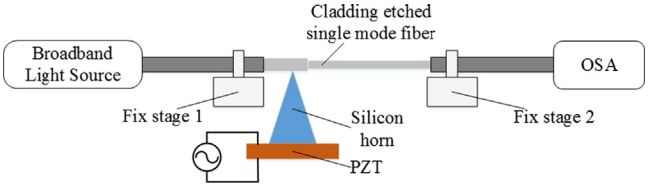

Fig. 1. The schematic for measurement of the CE-SMF-AOTF.

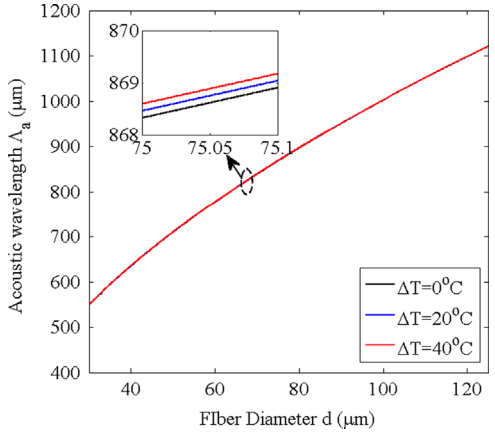

Fig. 2. Acoustic wavelength as a function of the fiber diameter for three different temperatures.

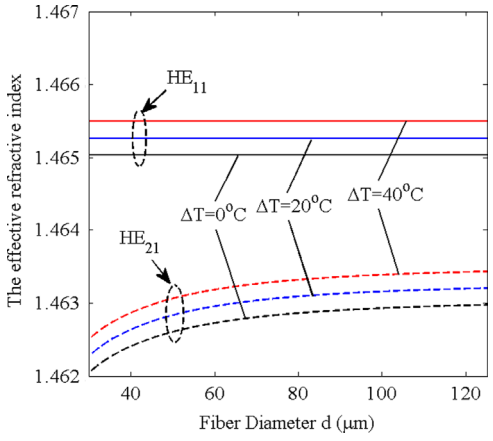

Fig. 3. The relationship between the effective refractive index of the fiber mode and the fiber diameter for three different temperatures.